HeartRhythm

The Official Journal of the Heart Rhythm Society, The Cardiac Electrophysiology Society, and The Pediatric & Congenital Electrophysiology Society

Heart Rhythm Society SM

Check for updates

Mapping the unseen: Programmed electrical stimulation to detect concealed conduction block

Rongheng Liao, MD,[1] Lu Zhang, MD,[1] Paul Knops, BSc,[1] Ziliang Ye, MD,[1] Yannick J.H.J. Taverne, MD, PhD,[2] Jolanda Kluin, MD, PhD,[2] Vehpi Yildirim, PhD,[1] Mathijs S. van Schie, PhD,[1] Antonio Frontera, MD, PhD,[3] Natasja M.S. de Groot, MD, PhD[1,4]

ABSTRACT

BACKGROUND Conduction blocks (CBs) play an important role in the initiation and perpetuation of atrial fibrillation and may be masked because of its direction- or rate dependency.

OBJECTIVE We aim to investigate how the highest amount and most severe CB at the right atrium (RA) can be unmasked by delivering programmed electrical stimulation (PES) from various directions and at different frequencies.

METHODS High-resolution epicardial mapping was performed at the middle of the RA on 40 patients during sinus rhythm (SR) and PES from the 4 sides of the mapping array at the average SR cycle length minus 50 ms (SR_{50}) and 3 different S1S2 trains ($S1_{400}$, $S2_{300}$, $S2_{250}$ or $S2_{200}$). CB area percentage (CBA%) was defined as the proportion of electrodes with a local conduction time $\geq$12 ms. CB severity was defined as the 95th percentile of the conduction times over the lines of CB.

RESULTS CBA% increased from 0.6 [0–7.0]% during SR to 15.4 [12.3–19.2]% during $S2_{200}$ ($P < .001$). CB severity increased from 18 [14–29] ms during SR to 46 [29–53] ms during $S2_{200}$ ($P < .001$). PES increased CBA% over SR from 58% of patients during SR_{50} to 100% during $S2_{200}$. The largest increase in CBA% occurred during $S2_{250}$ during pacing from perpendicular (+7.3 [0.5–10.8]%) and opposite (+7.4 [3.5–15.5]%) to the direction of SR.

CONCLUSION Perpendicular pacing opposite to the direction of SR using premature stimuli is optimal for unmasking CB. PES may also reduce CB in patients who already exhibit complex activation patterns during SR.

KEYWORDS Conduction abnormalities; Epicardial mapping; Programmed electrical stimulation; Pacing; Right atrium; Anisotropy; Atrial fibrillation

(Heart Rhythm 2026;23:e133–e141)

Conduction in cardiac tissue is anisotropic in nature, resulting in faster conduction along the longitudinal direction of the myocardial fibers compared with the transverse direction.[1] Structural remodeling often enhances conduction anisotropy and may cause areas of conduction slowing and conduction block (CBA), which potentially play a role in the initiation and perpetuation of atrial fibrillation (AF).[2,3] In previous mapping studies, we demonstrated that patients with AF episodes have indeed more and longer lines of CB during sinus rhythm (SR) compared with patients without AF.[4] However, the presence of conduction disorders may be underestimated as conduction disorders are both rate- and direction dependent because of tissue anisotropy.[5–8]

Rate- and direction-dependent conduction disorders may be unmasked by programmed electrical stimulation (PES) protocols consisting of different stimulation locations resulting in different wavefront propagation directions and cycle lengths of the pacing stimuli.

In patients with paroxysmal and persistent AF undergoing pulmonary vein isolation (PVI), recent data has suggested that conduction abnormalities present during either SR or pacing from the coronary sinus were related

From the [1]Department of Cardiology, Erasmus Medical Center, Rotterdam, The Netherlands, [2]Department of Cardiothoracic Surgery, Erasmus Medical Center, Rotterdam, The Netherlands, [3]Department of Cardiac Electrophysiology, Great Metropolitan Hospital Niguarda, Milan, Italy, and [4]Department of Microelectronics, Signal Processing Systems, Faculty of Electrical Engineering, Mathematics and Computer Sciences, Delft University of Technology, Delft, The Netherlands.

https://doi.org/10.1016/j.hrthm.2025.10.053

to AF recurrences after PVI. Based on their observations, the authors postulated that ablation of areas of (unmasked) CB may be novel target sites for AF ablation, which may reduce AF recurrences after PVI. Therefore, outcomes of this study indicate a potential clinical relevance for unmasking areas of conduction abnormalities using PES.[9] However, it is at the present unknown to what extent conduction disorders can be unmasked by applying different pacing protocols. Therefore, the goal of this study is to investigate (1) how the highest amount and most severe CB can be unmasked by PES from various directions and at different frequencies, and (2) the relationship between CBA during SR and PES. We only included patients without a history of atrial tachyarrhythmias to obtain thorough knowledge of the behavior of electrical properties to PES.

Methods

Study population

The study population consisted of 40 adult patients without a history of atrial tachyarrhythmias undergoing coronary artery bypass grafting (CABG), aortic or mitral valve surgery or a combination of valvular heart surgery and CABG in the Erasmus Medical Center Rotterdam. This study was approved by the institutional medical ethics committee (MEC2014-393) followed by ethical guidelines of the Declaration of Helsinki as revised in 2013. Written informed consent was obtained from all patients. Patient characteristics were retrieved from the patient's medical record.

Mapping procedure

Epicardial high-resolution mapping was performed prior to the commencement to extra-corporal circulation, as previously described in detail.[10] A steel wire fixed to the subcutaneous tissue of the thoracic cavity was used as an indifferent electrode. A 192-electrode array with 0.45 mm electrode diameter and 2.12 mm interelectrode distance was used for epicardial mapping of the middle part of the right atrium (RA), as illustrated in the upper left panel of Figure 1. The electrode array was positioned perpendicular to the terminal crest, 2 cm below the border of the superior caval vein. The mapping procedure started with recording 5 seconds of SR. Next, PES were delivered from distinct 4 sites surrounding the electrode array as shown in the upper left panel of Figure 1 and Supplemental Figure 1. PES included fixed rate pacing at the average SR cycle length minus 50 ms (SR_{50}) for 10 seconds, and premature stimulation (S1S2 trains; 5×S1: 400 ms [$S1_{400}$] followed by an S2: 300 [$S2_{300}$], 250 [$S2_{250}$] or 200 ms [$S2_{200}$]). Data were stored on a hard disk after amplification (gain 1000), filtering (bandwidth 0.5–400 Hz), sampling (1 kHz), and analog to digital conversion (16 bits).

Abbreviations

AF: atrial fibrillation

CB: conduction block

CBA: conduction block area

CT: conduction time

LAT: local activation time

PES: programmed electrical stimulation

RA: right atrium

Mapping data analysis

Unipolar electrograms (EGMs) were semi-automatically analyzed using custom-made software. The steepest negative slope of an atrial potential in the unipolar EGMs was marked as the local activation time (LAT) and used to construct color-coded activation maps. All annotations were manually checked with the consensus of 2 investigators. Only mapping locations from which more than 70% of the mapping area was available were included for analysis.

Lines of CB were defined as interelectrode activation time differences ≥12 ms.[2] Electrodes on both sides of the CB line were labeled as CB areas (CBA), as illustrated in the lower left panel of Figure 1. The prevalence of CBA% was defined as the proportion of electrodes with conduction time differences ≥12 ms relative to the total number of electrodes. CBA severity was defined as the 95th percentile of the conduction times histograms over the lines of CB. A change in CBA was considered as an increase or decrease when differences in CBA (ΔCBA) during various pacing sequences compared with SR were respectively >1% or <-1%.

Statistical analysis

The Shapiro-Wilk test was used to assess the normal distribution of continuous variables. For normally distributed continuous variables, results were presented using mean and standard deviation. Differences between groups were analyzed using repeated measures one-way ANOVA for data with repeated observations. For continuous variables that were not normally distributed, results were reported as median (25th–75th) or minimum and maximum. To evaluate differences between groups, the Friedman test and post hoc test was employed. Data analysis was performed using SPSS software (version 28) and R software (version 4.4.1). A $P < .05$ was considered statistically significant.

Results

Study population

Baseline characteristics of the study population (N = 40, 32 men (80.0%), age: 65.2 [43.3–75.4] years) are presented in Table 1. Patients had ischemic heart disease (N = 15, 37.5%), valvular heart disease (N = 21, 52.5%) or a combination of both conditions (N = 4, 10.0%). Most patients had normal left ventricular function (N = 32, 80.0%) and left atrial enlargement was present in 7 patients (17.5%). The average cycle length during SR was 936 ± 187 ms. SR_{50}, $S1_{400}$, $S2_{300}$, and $S2_{250}$ was captured from at least 1 pacing site in all patients. In only 9 patients (23%), there was a refractory period <250 ms in at least 1 of the 4 directions. Failure of capture because of atrial ectopy or refractoriness occurred in only 5% of the patients during $S1_{400}$, but increased to 15% during $S2_{250}$ and to 77% during $S2_{200}$, the shortest captured S1S2

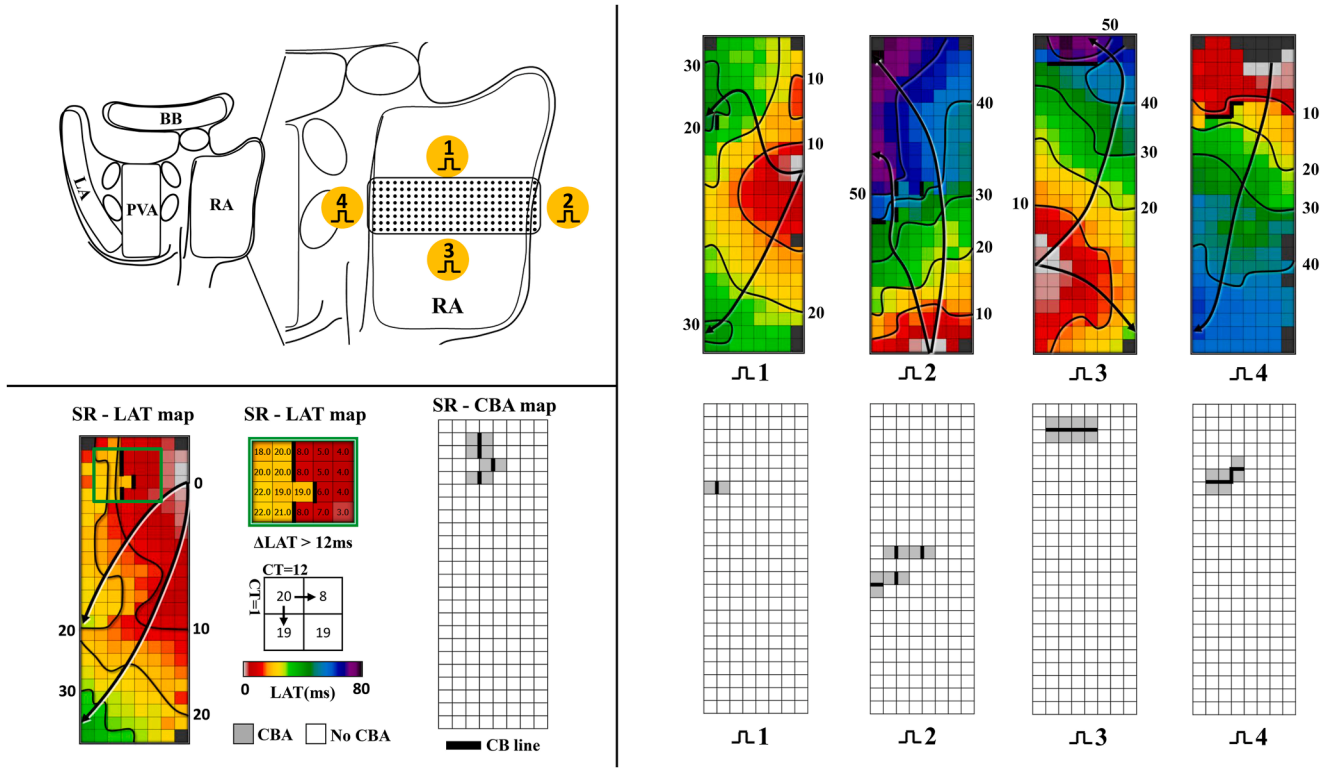

Figure 1

Mapping scheme and examples of activation maps during programmed electrical stimulation. Left upper panel: schematic presentation of the atria in a posterior view and position of the mapping array on the middle of right atrium. The numbers indicate the different pacing sites. Left lower panel: example of a color-coded activation map; isochrones (*black lines*) are drawn at 10 ms intervals and the *black arrow* indicates wavefront propagation. The *green rectangle* delineates a CB line (*thick black lines*). The CBA map shows this area in addition to adjacent electrodes on both sites of the *line* of CB (*gray squares*). The right panel demonstrated 4 activation maps and related conduction block area maps constructed during PES from the 4 different locations. BB = Bachmann bundle; CB = conduction block; CBA = conduction block area; CT = conduction time; LA = left atrium; LAT = Local activation time; PES = programmed electrical stimulation; PVA = pulmonary vein area; RA = right atrium; SR = sinus rhythm.

intervals at each location are provided in Supplemental Table 1.

Impact of PES on CBA

The left panel of Figure 2 illustrates the prevalence of CBA present during SR and each of the PES protocols separately. As expected, the median prevalence of CBA increased from 0.6 (0–7.0)% during SR to 4.4 (2.4–7.1)% during SR_{50} (P = .011). However, the prevalence of CBA did not differ between SR_{50} and $S1_{400}$ (4.4 [2.4–7.1] vs 4.5 [2.3–7.8]%, P = .750). The prevalence of CBA increased significantly during $S2_{300}$ to 5.7 (3.2–10.4)% (P = .002), to 10.2 (7.1–15.4)% during S_{250} (P < .001) and even to 15.4 (12.3–19.2)% during $S2_{200}$ (P < .001), as listed in Table 2. As illustrated in the right panel of Figure 2, the severity of CB also increased from 18 ms (14–29) during SR to ultimately 46 ms (29–53) during $S2_{200}$. Supplemental Figure 2 presents a patient with complete recordings for all PES protocols, in which PES was delivered in the opposite direction to SR. The prevalence of CBA increased from 4.9% during SR to 37.8% during $S2_{200}$ PES. However, the prevalence and severity of CBA during PES did not increase in all patients.

Figure 3 shows the proportion of patients in whom PES resulted in either an increase, decrease, or no change in CBA for each PES protocol for all 4 directions combined. The percentage of patients in whom the prevalence of CBA increased over SR was increased from 58% during SR_{50} to 100% during $S2_{200}$. In 24 patients, there was no CB during SR which increased during at least one of the pacing protocols. Interestingly, the prevalence of CBA did not change in 21% of the patients during SR_{50} and even decreased in 9% of patients during $S2_{250}$. During $S2_{250}$, the prevalence of CBA did not change over SR in 3% and decreased in 9% of the patients. Illustrations of activation maps with increased or decreased CBAs are provided in Figure 4. The left panel shows a CBA occurring during $S1_{400}$. In the right panel, there was a complex pattern of activation during SR because of CBA associated with an epicardial breakthrough. During $S1_{400}$, the mapping area was activated by 2 broad, uniform propagating wavefronts more or less perpendicular to the CBA and the CBA disappeared completely. Consequently, there was a lower prevalence of CBA. Therefore, PES resulted in a significant decrease in CBA.

Individual variation in response to PES

Inter-individual variation in CBA prevalence and severity over SR are illustrated in Figure 5. All patients were ranked according to differences in CBA prevalence (ΔCBA, left panel) or

Table 1 Baseline characteristics of the study population

Variables	Overall
Number of patients	40
Age, (median [IQR])	65.2 (43.3–75.4)
Men, n (%)	32 (80.0)
BMI, kg/m^2, mean (SD)	26.2 (4.1)
Underlying heart diseases	
IHD, n (%)	15 (37.5)
MVD, n (%)	1 (2.5)
AVD, n (%)	20 (50.0)
AVD + IHD, n (%)	4 (10.0)
Left ventricular function (%)	
Normal (EF >55%)	32 (80.0)
Mild impairment (EF 46%–55%)	6 (15.0)
Moderate impairment (EF 36%–45%)	2 (5.0)
Left atrial dilatation >45 mm, n (%)	7 (17.5)
Anti-arrhythmic drugs, n (%)	
Class I, n (%)	0 (0.0)
Class II, n (%)	29 (72.5)
Class III, n (%)	0 (0.0)
Class IV, n (%)	2 (5.0)

AVD = aorta valvular disease; EF = ejection factor; IHD = ischemic heart disease; MVD = mitral valvular disease.

CT_{95} (ΔCT_{95}, right panel) between SR and each of the PES protocols. As can be seen, inter-individual variation of ΔCBA was increased with pacing frequency. In general, $S2_{250}$ yielded the largest ΔCBA throughout all protocols since $S2_{200}$ could be only captured on 9 patients (23%) because of atrial refractoriness. There was no difference in absolute ΔCBA between patients with either an increase or decrease in absolute ΔCBA (SR_{50}: 2.7 [1.4–4.4]% versus 2.3 [0.3–3.8]% (P = .160), $S1_{400}$: 2.9 [1.9–4.8]% versus 2.6 [0.9–4.3]% (P = .322). Only when pacing at cycle lengths shorter than 300 ms, the ΔCBA in patients with an increase in CBA is higher than with a decrease in CBA ($S2_{300}$: 3.8 [2.2–7.2]% versus 0.9 [0.2–7.2]%, P = .003, $S2_{250}$: 3.5 [3.0–5.8]% versus 8.3 [4.9–10.8]%, P < .001). The severity of CB (ΔCT_{95}) during every pacing protocol is comparable, as can be seen in the right panel of Figure 5. During all PES protocols, there was no correlation between CBA prevalence and severity (r^2 < 0.012 and all P > .05).

Direction dependent CBA

The location of the pacing site had a large impact on CBA prevalence and severity, as summarized in Table 3. Except for $S1_{400}$ pacing (P = .151), ΔCBA differed considerably between pacing locations 1 and 3 and 2 and 4 (P < .005 for each). ΔCBAs in SR_{50} (N = 25), $S1_{400}$ (N = 17) and $S2_{200}$ (N = 2) protocols were higher when pacing from locations 1 and 3 compared with 2 and 4. However, during $S2_{300}$, $S2_{250}$ and $S2_{200}$ both the ΔCBA and ΔCT_{95} were higher during pacing from location 2 and 4 compared with location 1 and 3.

Figure 6 shows the complexity of direction-dependency of CBA. In the left panel, CBA was present in the distal part of the mapping array when stimulating from the location 2, which is perpendicular to SR activation direction but diminished when pacing from the opposite site (location 4), indicating a unidirectional CBA. In the middle panel, CBA was present during both pacing at locations 2 and 4, indicating a bidirectional CBA.

The right panel of Figure 6 illustrates the prevalence of CBA during pacing from the 4 different locations. As listed in Table 4, CBA particularly increased when PES was delivered from pacing locations 2 or 3, which is respectively perpendicular and opposite to SR activation direction. Specifically, SR_{50}, $S1_{300}$, $S2_{250}$ and $S2_{200}$ caused the largest increase in CBA when delivering PES from location 3. The

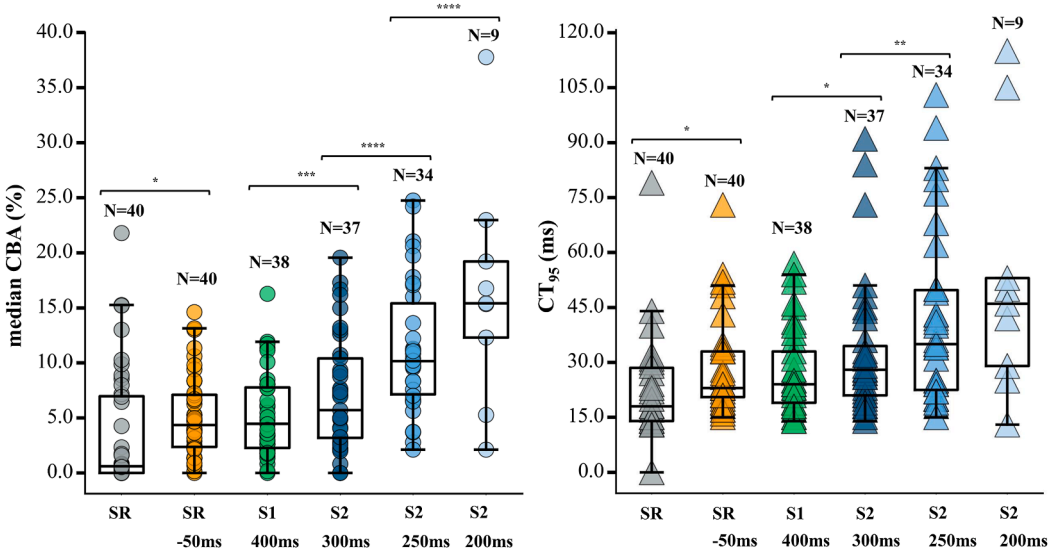

Figure 2
The prevalence of conduction block area (*dots*) and severity of CB (CT_{95}, *triangles*) during sinus rhythm and various PES protocols for each individual patient. Protocols are depicted by different colors, boxplots indicate median values, 25th percentile and 75th percentile. *P < .05, **P < .01, ***P < .005, ****P < .001
CBA = conduction block area; CT = conduction time; PES = programmed electrical stimulation; SR = sinus rhythm.

Table 2 Amount and severity of conduction block during various rhythms

Parameter	SR	SR_{50}	$S1_{400}$	$S2_{300}$	$S2_{250}$	$S2_{200}$
CBA (%)	0.6 [0–7.0]	4.4 [2.4–7.1]	4.5 [2.3–7.8]	5.7 [3.2–10.4]	10.2 [7.1–15.4]	15.4 [12.3–19.2]
CT_{95} (ms)	18 [14–29]	23 [20–33]	24 [19–33]	28 [21–34]	35 [23–49]	46 [29–53]

CBA = conduction block area; CT = conduction time; SR = sinus rhythm.

largest increase in CBA occurred during $S2_{250}$ from locations 2 (+7.3 [0.5–10.8]%) and 3 (+7.4 [3.5–15.5]%), $S2_{200}$ often did not capture because of atrial refractoriness.

Discussion

Key findings

The effect of different pacing strategies on unmasking both rate- and direction-dependent conduction disorders was systematically investigated for the first time. For this purpose, we used a high-resolution and density mapping technique. Our approach resulted in several important observations. Compared with SR, PES protocols not only increase, but may also decrease CBA, particularly when SR patterns of activation are complex, although a decrease in CBA induced by PES is less common throughout all protocols. When pacing from exact opposite directions, CBA can still be unidirectional. Pacing at SR_{50} yielded the same amount of CBA as pacing at 400 ms. As expected, shortening of the stimulation interval was not only associated with an increased amount of CBA, but also with an increase in severity of CB. Although most CBAs were recorded by delivering PES at $S2_{200}$, its efficacy was modest because of atrial refractoriness. $S2_{250}$ was most effective in unmasking the most severe CBA in most patients. Moreover, pacing locations, which were perpendicular and opposite to the direction of the SR wavefront yielded the highest amount and severity of CBA.

Conduction anisotropy

Conduction of electrical wavefronts is determined by tissue anisotropy which causes a lower conduction velocity in the transverse direction compared with the longitudinal direction.[1,6] Tissue anisotropy is the result of the cell shape of the cardiomyocytes, cell–cell connectivity, cell arrangement, and density of inter-cellular connections or branch sites of myocardial bundles.[11] Structural remodeling caused by, for example, aging and cardiovascular diseases enhances tissue anisotropy and induces conduction abnormalities, which is in turn associated with the development of AF.[12] It is, therefore, very likely that in structurally remodeled tissue, PES from different directions will unmask CBA.

Prior mapping studies demonstrated that conduction abnormalities during SR occur mainly at specific locations in the atria, including Bachmann's bundle,[13] and the superior part of the RA. At the superior RA, sinus node cells, blood vessels, or epicardial fat disrupts the muscular tissue, leading to impaired atrial conduction and a higher incidence of CBA.[14–17] We, therefore, selected the middle of the RA as a mapping location in the present study. Also, there is increasing evidence that the RA plays a role in the pathophysiology of AF.[4,14] In some patients, PES resulted in a continuous line of CB with a significant activation time delay between both sides of the CBA, which partly or completely disappeared when pacing from the opposite

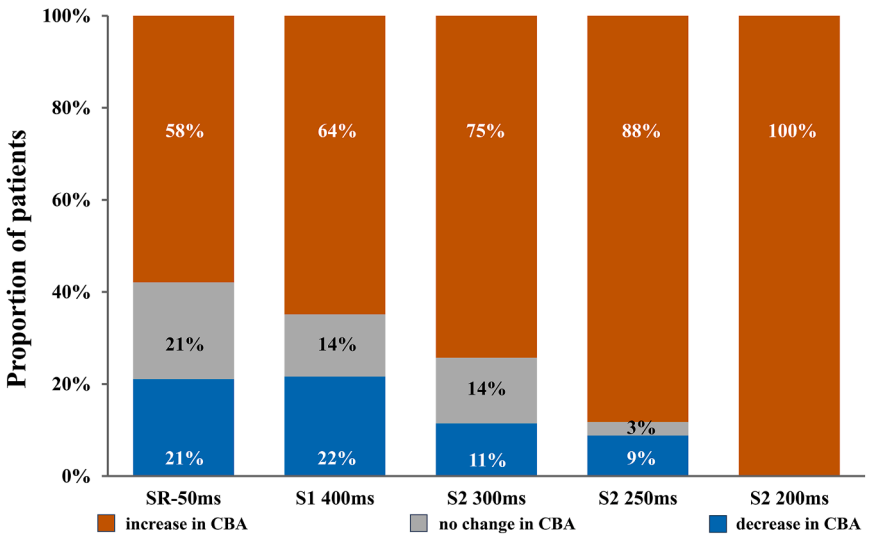

Figure 3
Stacked bars displaying the proportion of patients in whom PES resulted in either an increase (*orange*), decrease (*blue*) or no change (*gray*) in conduction block area during the various PES protocols for all 4 directions combined. CBA = conduction block area; PES = programmed electrical stimulation; SR = sinus rhythm.

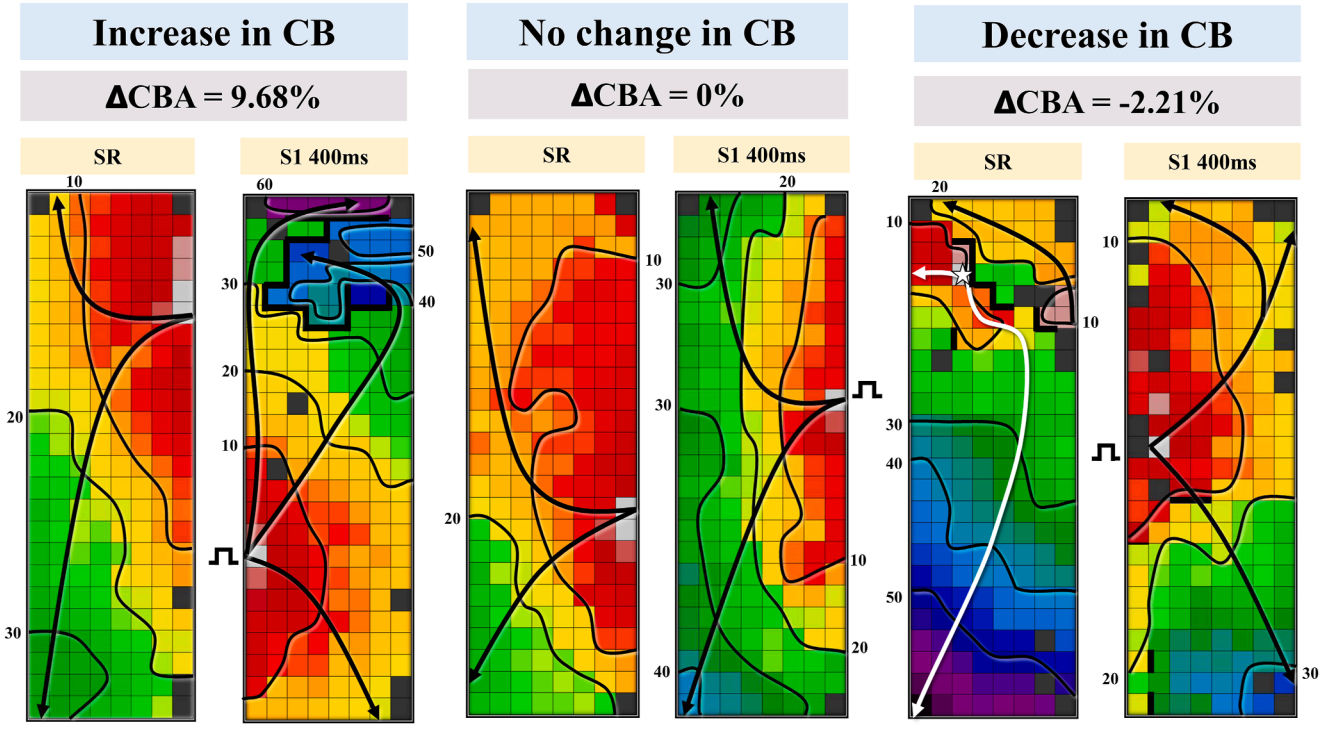

Figure 4
Examples of local activation time (LAT) maps of patients in whom PES resulted in either an increase (left panel), decrease (right panel) or no change (middle panel) in the prevalence of CBA. For each example, an activation maps from sinus rhythm (left) and corresponding S1 pacing (right) are demonstrated. Isochrones (*black lines*) are drawn at 10 ms intervals, the *black arrow* indicates wavefront propagation and thick black lines indicate CBA. CB = conduction block; PES = programmed electrical stimulation; SR = sinus rhythm.

direction. This can be explained by the absence of a transmural CBA, which reflects the complex 3-dimensional structure of the atrial wall. Prior simultaneous endo-epicardial mapping studies of the right atrial wall have demonstrated the presence of non-transmural CBA during SR.[14,18] At present, differences in contribution of these transmural or non-transmural CBA to AF pathophysiology are unknown.

Mapping during spontaneous extrasystoles

In recent epicardial mapping studies, it was demonstrated that spontaneous atrial extrasystoles (AES) unmasked the largest proportion of conduction abnormalities when the propagation direction was perpendicular to that of the SR wavefront,[19,20] unipolar potential characteristics were mainly direction-dependent but not rate-dependent. At all atrial

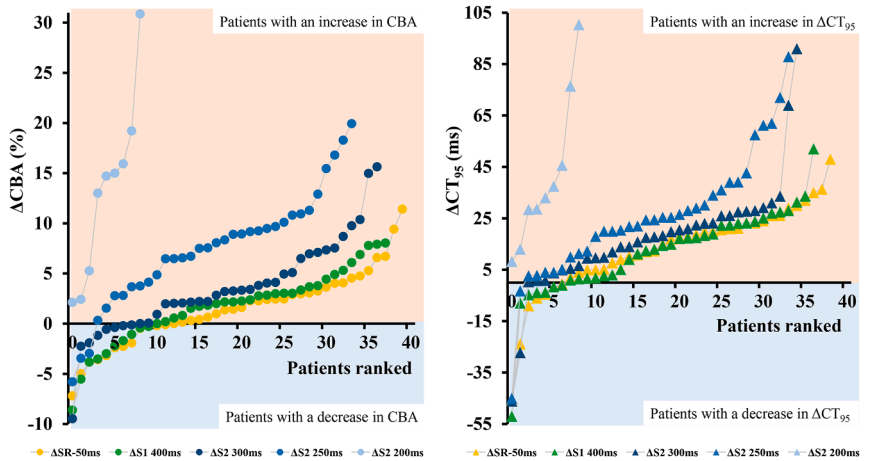

Figure 5
Differences in prevalence of CBA prevalence (left panel) and CBA severity (right panel) between SR and the various PES protocols are plotted for each individual patient. Patients are ranked according to increasing differences in CBA or CT_{95}. A positive or negative change in CB (severity) is indicated by respectively an *orange* or *blue* background. CBA = conduction block area; CT = conduction time; PES = programmed electrical stimulation; SR = sinus rhythm.

Table 3 Difference between SR and the various of PES directions

Parameter	SR_{50}-SR	$S1_{400}$-SR	$S2_{300}$-SR	$S2_{250}$-SR	$S2_{200}$-SR
ΔCBA (%) loc 1–3	+1.9 [0–4.2]	+2.0 [−0.3 to 3.3]	+2.7 [0.6–6.2]	+6.8 [3.1–10.6]	+30.5 [13.0–30.9]
ΔCBA (%) loc 2–4	+0.9 [−0.5 to 3.3]	+1.1 [−0.4 to 3.3]	+3.4 [0.0–6.4]	+7.0 [0.6–9.6]	+6.4 [3.8–12.6]
P-value	.005	.151	<.001	.002	<.001
ΔCT_{95} (ms) loc 1–3	+6 [0–19]	+5 [2–16]	+5 [1–19]	+13 [4–41]	+57 [31–82]
ΔCT_{95} (ms) loc 2–4	+3 [0–8]	+2 [−4 to 5]	+8 [4–14]	+7 [0–21]	+31 [23–50]
P-value	<.001	<.001	<.001	<.001	<.001

CBA = conduction block area; CT = conduction time; SR = sinus rhythm.

regions, spontaneous AES decreased potential voltages, increased the amount of low-voltage areas, and increased the degree of potential fractionation; potential morphology was mostly affected by wavefronts propagating in opposite direction compared with the SR wavefront. AF patients have more direction-dependent conduction disorders, indicating enhanced non-uniform anisotropy that is uncovered by spontaneous AES.[21] However, these spontaneous AES do not reach the refractory period so an even larger effect of short-coupled AES can be expected when the wavefront approaches the refractory period. Frontera et al. recently demonstrated that pacing from the coronary sinus with a coupling interval of +30 ms greater than the local effective refractory period revealed conduction disorders, which were strongly related to AF recurrences after PVI.[9] The coupling interval used in this study is comparable to the PES protocol ($S2_{250}$) which yielded the largest amount of CBA in the present study, as most of our patients had reached atrial refractoriness at 200 ms. In some patients, CBA decreased during PES protocols when a complex pattern of activation caused by an epicardial breakthrough wave was already present during SR. In this case, PES induced a more uniform activation pattern in the epicardial plane, resulting in a lower CBA compared with SR. Different degrees of structural or electrical remodeling caused by different underlying cardiovascular diseases contributes to inter-individual differences in the amount of unmasked CBA. Additionally, more caudally located sinus node exit sites may be blocked by PES resulting in different activation pathways, and therefore, a different amount of CBA.[22]

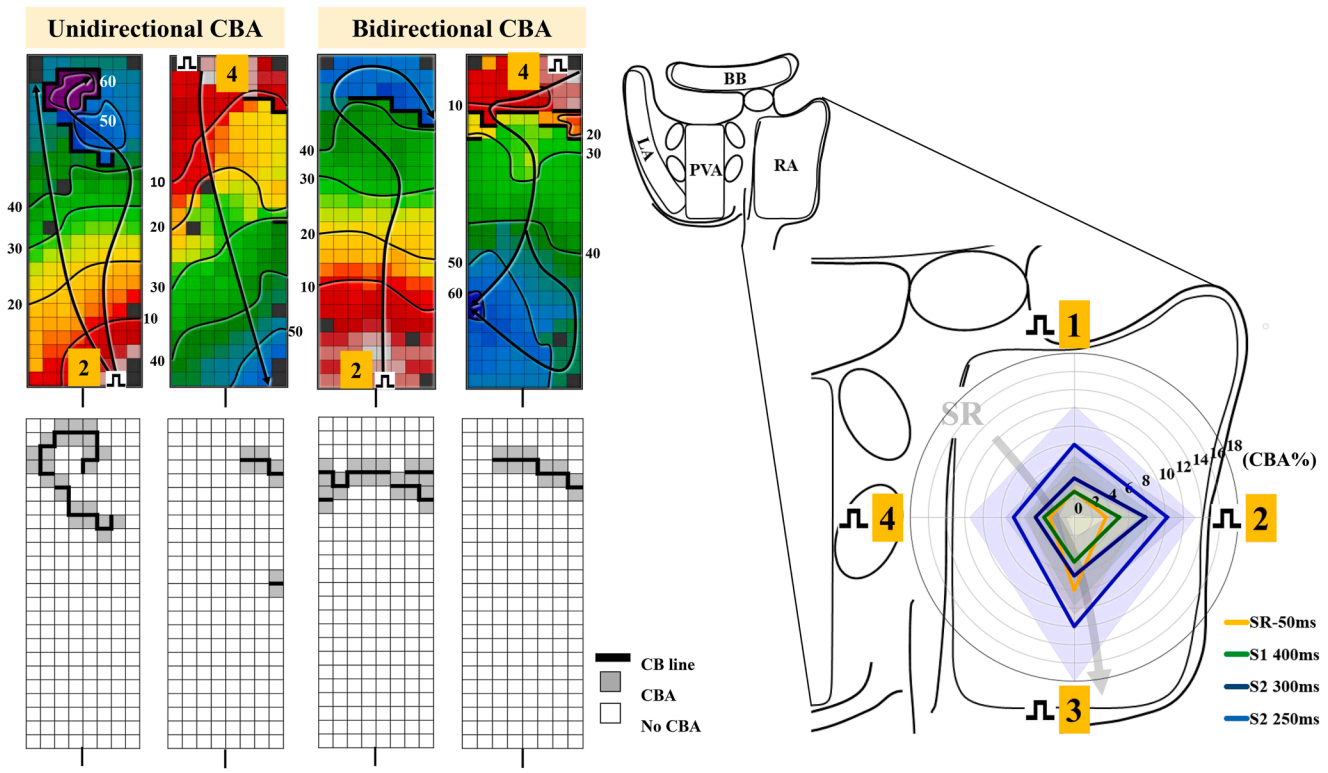

Figure 6
Impact of activation direction on CBA. The left panel demonstrates local activation time (LAT) maps with a unidirectional CBA and bidirectional CBA and corresponding CBA maps. The right panel shows the prevalence of CBA during PES from the 4 different directions. Propagation of the sinus rhythm wavefront is indicated by a *gray arrow*. BB = Bachmann bundle; CB = conduction block; CBA = conduction block area; LA = left atrium; PES = programmed electrical stimulation; PVA = pulmonary vein area; RA = right atrium; SR = sinus rhythm.

Table 4 Differences between SR and the various PES locations

Parameter	SR_{50}-SR	$S1_{400}$-SR	$S2_{300}$-SR	$S2_{250}$-SR	$S2_{200}$-SR
ΔCBA (%) loc 1	+0.3 [-0.9 to 4.1]	+1.6 [-0.5 to 4.0]	+2.6 [-0.3 to 6.3]	+5.8 [2.4–9.6]	+21.8 [13.0–30.1]
ΔCBA (%) loc 2	+0.5 [-1.4 to 3.1]	+0.5 [-0.8 to 3.5]	+2.1 [-0.7 to 8.1]	+7.3 [0.5–10.8]	+3.8 [2.0–16.4]
ΔCBA (%) loc 3	+2.9 [1.4–7.6]	+1.2 [-0.8 to 5.4]	+2.8 [-0.2 to 8.4]	+7.4 [3.5–15.5]	+15.4 [12.4–31.2]
ΔCBA (%) loc 4	+0.7 [-0.5 to 3.2]	+1.0 [-0.4 to 3.3]	+1.8 [0.0–6.6]	+6.2 [1.2–11.3]	+11.7
P-value	<.001	<.001	<.001	<.001	.005
ΔCT_{95} (ms) loc 1	+4 [-3 to 16]	+8 [-1 to 16]	+13 [-1 to 23]	+12 [0–20]	+27 [8–46]
ΔCT_{95} (ms) loc 2	+2 [-6 to 17]	+3 [-3 to 13]	+12 [2–19]	+14 [3–23]	+29 [10–50]
ΔCT_{95} (ms) loc 3	+16 [3–22]	+9.7 [-4 to 19]	+14 [-2 to 23]	+20 [10–42]	+77 [38–100]
ΔCT_{95} (ms) loc 4	+8 [2–18]	+1.3 [-2 to 15]	+9 [-0.1 to 16.2]	+15 [4–34]	+15 [7–23]
P-value	<.001	<.001	.009	<.001	.002

CBA = conduction block area; CT = conduction time; SR = sinus rhythm.

Direction and frequency dependent PES

Experimental and clinical studies have demonstrated that conduction abnormalities in the RA are dependent on pacing direction and frequency.[21,23,24] In the RA, Mitsuru et al. showed that pacing at the coronary sinus ostium resulted in a significantly higher prevalence of CB compared with pacing at the low lateral RA. Additionally, higher pacing frequencies at both sites also resulted in higher CB prevalence.[25] Thus, these observations are in line with our findings that pacing from the inferior parts of the RA, opposite to the SR activation direction, effectively unmasks conduction abnormalities.

Interestingly, in some patients, specific pacing protocols reduced the amount and severity of conduction abnormalities compared with SR. This occurred when there was already a complex pattern of activation present during SR, consisting of epicardial breakthrough waves and large CBA. Comparison of SR and paced activation maps are thus essential to fully understand the impact of PES and therefore, accurate identification of the AF-related arrhythmogenic substrate.

PES used in unmasking hidden conduction abnormalities was first demonstrated during ventricular mapping. In these studies, S1S2 or S1S2S3 stimulation was respectively performed at multiple sites on the right ventricle using different pacing protocols.[26,27] Hikmet et al. investigated functional slow conduction areas revealed by PES from the coronary sinus, which were related to recurrence of atrial tachyarrhythmia during follow-up.[26] Similarly, Frontera et al. also investigated so-called 'functional rhythm-dependent conduction abnormalities' present during either SR or PES, and the complex interrelationship between CBA during SR and PES observed in our study supports this approach.[9] They also demonstrated that these functional rhythm-dependent conduction abnormalities were associated with AF recurrences after PVI. Therefore, their study emphasized the clinical importance of accurately unmasking conduction abnormalities to identify potential arrhythmogenic substrates underlying AF, and thus also the need to select the most optimal pacing location and frequency. To further improve this methodology, we demonstrated that dedicated PES techniques, which have the advantage of providing a stable and repetitive heart rhythms, delivering stimuli close to the refractory period at specific location, particularly opposite to the SR wavefront propagation direction, can be used to unmask concealed CBAs.

Clinical perspective

At present, it is still unknown what the most optimal ablation approach of AF recurrences is when the pulmonary veins are isolated. Recently, findings from Frontera et al. suggested that unmasked functional rhythm-dependent conduction abnormalities were related to AF recurrences after PVI.[9] These findings suggest that areas of conduction slowing/block play a role in the pathophysiology of AF recurrences and may be potential target sites beyond PVI. Our study systematically investigated how concealed CBA can be unmasked and which PES strategies are most effective for this purpose. More studies are needed to demonstrate which type and which severity of conduction abnormalities play a role in initiation and/or perpetuation of the fibrillatory process in patients with AF, and that ablation of these sites reduces AF recurrences, before considering these sites as target sites for AF ablation.

Limitations

Owing to practical issues, it was not always possible to perform the PES protocol from every location. PES protocols were performed exclusively on the epicardial layer of the RA, However, we previously demonstrated that there are no differences in electrical properties between the endo- and epicardium.[28] Correlations with magnetic resonance imaging (MRI) could not be made as MRI images were not available in every patient and pre-operative MRI images cannot be accurately correlated with intra-operative high-resolution mapping images.

Conclusion

A higher number of CBs can be demonstrated with premature electrical stimulation delivered from a site opposite or perpendicular to the SR wavefront. The severity of CB can be highlighted using a fast drive train ($S1_{400}$) shortest possible coupling interval for the extra stimulus, which is most often $S2_{250}$. Future studies are required to unravel the

inter-relationship between different types of CBA occurring during SR and/or PES and AF pathophysiology. Unmasking CBA is important as they may play role in initiation or perpetuation in AF.

Acknowledgments

The authors thank J.A. Bekkers, MD; W.J. van Leeuwen, MD; F.B.S. Oei, MD, PhD; P.C. van de Woestijne, MD; F.R.N. van Schaagen, MD; M.C. Roos-Serote, PhD for their contribution to this work.

Appendix

Supplementary data

Supplementary data associated with this article can be found in the online version at https://doi.org/10.1016/j.hrthm.2025.10.053.

Funding Sources: N.M.S. de Groot, MD, PhD is supported by funding grants from CVON-AFFIP (grant number 914728), NWO-Vidi (grant number 91717339), Biosense Webster Inc., part of Johnson & Johnson MedTech (ICD 783454) and Medical Delta.

Disclosures: The authors have no conflicts of interest to disclose.

Data Availability: Data from this article will be shared on reasonable request to the corresponding author.

Address reprint requests and correspondence: Dr N.M.S de Groot, Unit Translational Electrophysiology, Department of Cardiology, Erasmus Medical Center, Dr. Molewaterplein 40, 3015GD Rotterdam, The Netherlands. E-mail address: n.m.s.degroot@erasmusmc.nl

References

1. Kléber AG, Rudy Y. Basic mechanisms of cardiac impulse propagation and associated arrhythmias. Physiol Rev 2004;84:431–488.
2. Allessie MA, de Groot NM, Houben RP, et al. Electropathological substrate of long-standing persistent atrial fibrillation in patients with structural heart disease: longitudinal dissociation. Circ Arrhythm Electrophysiol 2010; 3:606–615.
3. Frontera A, Pagani S, Limite LR, et al. Slow conduction corridors and pivot sites characterize the electrical remodeling in atrial fibrillation. JACC Clin Electrophysiol 2022;8:561–577.
4. Heida A, van der Does WFB, van Staveren LN, et al. Conduction heterogeneity: impact of underlying heart disease and atrial fibrillation. JACC Clin Electrophysiol 2020;6:1844–1854.
5. Rohr S, Kucera JP, Kléber AG. Slow conduction in cardiac tissue, I: effects of a reduction of excitability versus a reduction of electrical coupling on microconduction. Circ Res 1998;83:781–794.
6. Spach MS, Kootsey JM, Sloan JD. Active modulation of electrical coupling between cardiac cells of the dog. A mechanism for transient and steady state variations in conduction velocity. Circ Res 1982;51:347–362.
7. Kawara T, Derksen R, de Groot JR, et al. Activation delay after premature stimulation in chronically diseased human myocardium relates to the architecture of interstitial fibrosis. Circulation 2001;104:3069–3075.
8. Punske BB, Taccardi B, Steadman B, et al. Effect of fiber orientation on propagation: electrical mapping of genetically altered mouse hearts. J Electrocardiol 2005;38(suppl):40–44.
9. Frontera A, Villella F, Cristiano E, et al. The functional substrate in patients with atrial fibrillation is predictive of recurrences following catheter ablation. Heart Rhythm 2025;22:1401–1410.
10. Yaksh A, van der Does LJ, Kik C, et al. A novel intra-operative, high-resolution atrial mapping approach. J Interv Card Electrophysiol 2015;44:221–225.
11. Spach MS, Dolber PC, Heidlage JF. Influence of the passive anisotropic properties on directional differences in propagation following modification of the sodium conductance in human atrial muscle. A model of reentry based on anisotropic discontinuous propagation. Circ Res 1988; 62:811–832.
12. Ho SY. Normal and abnormal atrial anatomy relevant to atrial flutters: areas of physiological and acquired conduction blocks and delays predisposing to re-entry. Card Electrophysiol Clin 2022;14:375–384.
13. Teuwen CP, Yaksh A, Lanters EA, et al. Relevance of conduction disorders in Bachmann's bundle during sinus rhythm in humans. Circ Arrhythm Electrophysiol 2016;9:e003972.
14. Kharbanda RK, Knops P, van der Does LJME, et al. Simultaneous endo-epicardial mapping of the human right atrium: unraveling atrial excitation. J Am Heart Assoc 2020;9:e017069.
15. Fedorov VV, Glukhov AV, Chang R, et al. Optical mapping of the isolated coronary-perfused human sinus node. J Am Coll Cardiol 2010;56:1386–1394.
16. Jongbloed MR, Vicente Steijn R, Hahurij ND, et al. Normal and abnormal development of the cardiac conduction system; implications for conduction and rhythm disorders in the child and adult. Differentiation 2012;84:131–148.
17. Sánchez-Quintana D, Cabrera JA, Farré J, Climent V, Anderson RH, Ho SY. Sinus node revisited in the era of electroanatomical mapping and catheter ablation. Heart 2005;91:189–194.
18. Zhang L, van Schie MS, Xiang H, et al. Identification of atrial transmural conduction inhomogeneity using unipolar electrogram morphology. J Clin Med 2024; 13:1015.
19. Teuwen CP, Kik C, van der Does LJME, et al. Quantification of the arrhythmogenic effects of spontaneous atrial extrasystole using high-resolution epicardial mapping. Circ Arrhythm Electrophysiol 2018;11:e005745.
20. van Schie MS, Liao R, Ramdat Misier NL, et al. Atrial extrasystoles enhance low-voltage fractionation electrograms in patients with atrial fibrillation. Europace 2023;25:euad223.
21. Starreveld R, de Groot NMS. Direction- and rate-dependent fractionation during atrial fibrillation persistence: unmasking cardiac anisotropy? J Cardiovasc Electrophysiol 2020;31:2206–2209.
22. Kalyanasundaram A, Li N, Augostini RS, Weiss R, Hummel JD, Fedorov VV. Three-dimensional functional anatomy of the human sinoatrial node for epicardial and endocardial mapping and ablation. Heart Rhythm 2023; 20:122–133.
23. Berenfeld O, Zaitsev AV. The muscular network of the sheep right atrium and frequency-dependent breakdown of wave propagation. Anat Rec A Discov Mol Cell Evol Biol 2004;280:1053–1061.
24. Hardebeck CJ. Electrocardiographic characteristics of pacing from the right atrial appendage during atrioventricular sequential pacing. Pacing Clin Electrophysiol 1988;11:193–202.
25. Takami M, Yoshida A, Fukuzawa K, et al. Rate-dependent and site-specific conduction block at the posterior right atrium and drug effects evaluated using a noncontact mapping system in patients with typical atrial flutter. J Cardiovasc Electrophysiol 2012;23:827–834.
26. de Riva M, Naruse Y, Ebert M, et al. Targeting the hidden substrate unmasked by right ventricular extrastimulation improves ventricular tachycardia ablation outcome after myocardial infarction. JACC Clin Electrophysiol 2018; 4:316–327.
27. Guichard JB, Regany-Closa M, Vázquez-Calvo S, et al. Substrate mapping for ventricular tachycardia ablation through high-density whole-chamber double extra stimuli: the S3 protocol. JACC Clin Electrophysiol 2024; 10:1534–1547.
28. van der Does LJME, Knops P, Teuwen CP, et al. Unipolar atrial electrogram morphology from an epicardial and endocardial perspective. Heart Rhythm 2018;15:879–887.